

Impact mixing among rocky planetesimals in the early Solar System from angrite oxygen isotopes

Rider-Stokes, B. G.; Greenwood, Richard C.; Anand, M.; White, L. F.; Franchi, Ian A.; Debaille, Vinciane; Goderis, S.; Pittarello, Lidia; Yamaguchi, Akira; Mikouchi, T.; Claeys, Philippe

Published in:
Nature Astronomy

DOI:
[10.1038/s41550-023-01968-0](https://doi.org/10.1038/s41550-023-01968-0)

Publication date:
2023

License:
Other

Document Version:
Accepted author manuscript

[Link to publication](#)

Citation for published version (APA):

Rider-Stokes, B. G., Greenwood, R. C., Anand, M., White, L. F., Franchi, I. A., Debaille, V., Goderis, S., Pittarello, L., Yamaguchi, A., Mikouchi, T., & Claeys, P. (2023). Impact mixing among rocky planetesimals in the early Solar System from angrite oxygen isotopes. *Nature Astronomy*, 7(7), 836-842. [1968].
<https://doi.org/10.1038/s41550-023-01968-0>

Copyright

No part of this publication may be reproduced or transmitted in any form, without the prior written permission of the author(s) or other rights holders to whom publication rights have been transferred, unless permitted by a license attached to the publication (a Creative Commons license or other), or unless exceptions to copyright law apply.

Take down policy

If you believe that this document infringes your copyright or other rights, please contact openaccess@vub.be, with details of the nature of the infringement. We will investigate the claim and if justified, we will take the appropriate steps.

1 **Outward displacement of rocky planetesimals in the early Solar System: Oxygen isotope**
2 **evidence from angrites.**

3
4 Rider-Stokes, B. G.¹, Greenwood, R. C.¹, Anand, M.^{1,2}, White, L. F.¹, Franchi, I. A.¹,
5 Debaille, V.³, Goderis, S.⁴, Pittarello, L.^{5,6}, Yamaguchi, A.⁷ & Mikouchi, T.⁸, & Claeys, P.⁴.

6
7 ¹*School of Physical Sciences, The Open University, Milton Keynes, MK7 6AA, UK. *Corresponding Author;*
8 ben.rider-stokes@open.ac.uk ²*Department of Mineralogy, The Natural History Museum, London, SW7 5BD,*
9 *UK. ³Laboratoire G-Time, Université Libre de Bruxelles, CP 160/02, 50, Av. F.D. Roosevelt, 1050, Brussels,*
10 *Belgium. ⁴Department of Chemistry, Vrije Universiteit Brussel, Pleinlaan 2, 1050, Brussels, Belgium.*
11 ⁵*Naturhistorisches Museum Wien, Mineralogisch-Petrographische Abteilung, Burgring 7,A-1010 Vienna,*
12 *Austria. ⁶University of Vienna, Department of Lithospheric Research, Althanstrasse 14, A-1090 Vienna,*
13 *Austria. ⁷National Institute of Polar Research, Tachikawa, Tokyo 190-8518, Japan. ⁸Department of Earth and*
14 *Planetary Science, The University of Tokyo, 7-3-1 Hongo, Bunkyo-ku Tokyo, 113-0033 Japan.*
15

16 **Angrite meteorites are ancient inner Solar System meteorites that likely formed**
17 **inward of Jupiter’s orbit based on their isotopic parameters such as $\epsilon^{50}\text{Ti}$ vs $\epsilon^{54}\text{Cr}$ and**
18 **$\Delta^{17}\text{O}$ vs $\epsilon^{54}\text{Cr}$ in addition to Fe/Mn ratios of pyroxene^{1,2}. Angrites therefore provide a**
19 **unique insight into the earliest stages of planetary evolution in the inner Solar System.**
20 **Here, we report the bulk oxygen isotope composition of nine angrite meteorites, as well**
21 **as olivine xenocrysts and matrix fractions from three “quenched” angrites. We calculate**
22 **a new average $\Delta^{17}\text{O}$ value for bulk angrites, which overlaps with the $\Delta^{17}\text{O}$ results of**
23 **terrestrial materials when treated in the same manner, hence supporting the proposition**
24 **that angrites and Earth may be derived from a similar precursor reservoir². Our analyses**
25 **of olivine xenocrysts and matrix fractions from Asuka 12209, Asuka 881371 and NWA**
26 **12320 define a clear isotopic disequilibrium, with matrix fractions yielding higher $\Delta^{17}\text{O}$**
27 **values than either the xenocrysts or bulk samples. Microstructural investigations of NWA**
28 **12320 reveal the presence of both fully recrystallized and undeformed olivine xenocrysts,**
29 **indicating that some xenocrysts underwent high temperature events. We interpret these**
30 **findings in terms of angrite meteorites recording evidence of impact-driven isotopic**
31 **mixing, possibly in response to early giant planet migration.**

32
33 *Key words: Angrites; Oxygen Isotopes; Laser Fluorination; Early Solar System Processes;*
34 *EBSD; Angrite Fractionation Line.*

35 Angrites constitute a group of unshocked, alkali-depleted basaltic meteorites that are
36 amongst the oldest igneous rocks in the Solar System^{3,4}. Based on the mineral chemistry of
37 pyroxene (Fe/Mn ratios) within angrites, it has been suggested that their parent body (APB)
38 originated from a similar planetary reservoir to that of the Earth-Moon system². Evidence from
39 Mn/Cr isotopic systematic indicates that the APB was larger than 4 Vesta⁵. On the basis of
40 differing textures and mineralogy, angrites have been principally divided into plutonic angrites
41 (slowly-cooled) with crystallisation ages ranging from 4560.74 ± 0.47 to 4556.60 ± 0.26 Ma
42 and quenched angrites with crystallisation ages ranging from 4564.39 ± 0.24 to 4562.2 ± 0.7
43 Ma (rapidly-cooled) subgroups⁵. However, there are some angrites, with similar mineralogical
44 assemblages yet differing textures, which do not fit into either of these categories. For example,
45 Northwest Africa (NWA) 8535 has been classified as a dunite (early formed cumulate) and
46 NWA 10463 represents an intermediate stage between the plutonic and quenched angrites,
47 which has recently been dated to 4560.25 ± 0.18 Ma^{6,7}.

48

49 The oxygen isotope composition of bulk angrites display a high level of homogeneity,
50 particularly with regards to ¹⁷O-excess ($\Delta^{17}\text{O}$), indicating that all the currently identified
51 angritic meteorites originated from a single parent body (APB) and likely underwent early
52 isotopic homogenisation in a global magma ocean^{8,9}. Although many angrites display limited
53 evidence of shock deformation, indicating that the APB was not affected by significant impact
54 processing¹⁰, it has been suggested that the quenched angrites may represent impact melts^{11,12}.
55 While this hypothesis has been disputed³, the recent discovery of variable deformation features
56 in olivine xenocrysts within Asuka 881371 and Asuka 12209 further supports the impact
57 hypothesis^{13,14}, whereby olivine xenocrysts are relict grains originating from areas of the APB
58 that survived impact melting¹³. However, it has also been argued that the kink bands and sub-
59 grain boundary formation in olivine grains could result from ductile deformation in the APB
60 mantle¹⁴. Consequently further evidence is required to constrain the petrogenesis of the
61 quenched angrites.

62

63 We collected high-precision, three O isotope data on bulk-rock samples from nine
64 angrites, encompassing all petrologic subgroups (see supplementary for further details), using
65 laser-assisted fluorination following established procedures^{9,15}. In addition, separated olivine
66 and matrix fractions from Asuka 881371, Asuka 12209, and NWA 12320 were also analysed.
67 All samples were treated with a solution of ethanolamine thioglycollate (EATG) to ensure that
68 any isotopic variations were not a result of terrestrial contamination (see supplementary

69 details). All uncertainties are reported at 2SD and $N = 2$ for all individual sample averages,
70 where 1 N equals four blocks of ten measurements .

71

72 While the oxygen isotopic compositions ($\Delta^{17}\text{O} = \delta^{17}\text{O} - 0.52 \times \delta^{18}\text{O}$) for five angrites
73 have been previously reported as homogenous ($\Delta^{17}\text{O} = -0.072 \pm 0.014\text{‰}$), we observe that
74 the whole-rock $\Delta^{17}\text{O}$ value of NWA 12320 ($\Delta^{17}\text{O} = -0.017 \pm 0.004\text{‰}$) and matrix fractions
75 of NWA 12320, Asuka 12209 and Asuka 881371 reveal less negative values that are
76 statistically distinct from the other angrite meteorites ($\Delta^{17}\text{O} = -0.024 \pm 0.016\text{‰}$, $-0.001 \pm$
77 0.007‰ and $-0.003 \pm 0.007\text{‰}$, respectively). Intriguingly, the olivine xenocrysts in NWA
78 12320, Asuka 12209 and Asuka 881371 display $\Delta^{17}\text{O}$ values of $-0.065 \pm 0.018\text{‰}$, $-0.068 \pm$
79 0.015‰ and $-0.067 \pm 0.008\text{‰}$, respectively, indistinguishable from the other whole-rock
80 angrite meteorites (Figure 1). These results indicate that the matrix in NWA 12320, Asuka-
81 12209 and Asuka-881371 are isotopically distinct from the rest of the samples. While lesser
82 amounts of matrix may result in undetectable shifts in some quenched angrites, NWA 12320
83 is dominated by matrix and therefore the whole-rock sample equates to a matrix separate. The
84 origin of such isotopic heterogeneity within magmatic samples requires addition of isotopically
85 distinct material and therefore to calculate an AFL, we have opted to incorporate the $\Delta^{17}\text{O}$
86 values of the olivine xenocrysts in NWA 12320, Asuka 12209 and Asuka 881371 while
87 excluding their matrix fractions and the whole-rock value of NWA 12320. From this, we derive
88 an average $\Delta^{17}\text{O}$ value of $-0.065 \pm 0.016\text{‰}$, redefining the AFL utilising eleven individual
89 samples. All whole-rock measurements reported here, excluding the NWA 12320 datum, fall
90 within uncertainty of this new AFL, providing considerable evidence that angrites are
91 homogenous in regard to $\Delta^{17}\text{O}$ and suggesting that angrite meteorites all originate from a single
92 differentiated parent body that was homogeneous with respect to oxygen isotopes.

93

94 A complex history of the xenocrysts in NWA 12320 is apparent from contrasting
95 internal structures revealed by electron backscatter diffraction (EBSD) and point to two distinct
96 populations of olivine xenocrysts, one of which has a granular texture, clearly illustrated by
97 band contrast images and inverse pole figures (IPF) (Figure 2). The granular olivine xenocrysts
98 have no discernible preferred orientation and are cemented by olivine with a higher Fe content,
99 with each neighbouring grains displaying vastly distinct orientations. This is indicative of
100 recrystallization, after shock-induced mosaicism or fragmentation. A second population of
101 olivine xenocrysts demonstrates unaltered, undeformed grains with little to no internal
102 misorientation (Figure 2). A similarly complex history for the xenocrysts within Asuka 12209

103 is exhibited by various degrees of lattice deformation, from weak deformation bands to
104 subgrain rotation crystallization (see supplementary for further details).

105

106 The granular textures seen in NWA 12320 resemble experimental recrystallization
107 textures induced at 1000 °C under dynamic conditions¹⁶, but are also similar to polycrystalline
108 olivine identified in the howardite impact melt breccia Jiddat al Harasis 556¹⁷ and the ureilite
109 impact melt breccia Jiddat al Harasis 422¹⁸. Most noticeably, there is a measurable oxygen
110 isotope variation between the matrix and whole-rock values for both samples, similar to the
111 quenched angrite meteorites. The authors of these two studies^{17,18} conclude that the olivine
112 xenocrysts represent relict grains that underwent recrystallisation in the impact melt. This
113 indicates that at least some olivine grains in NWA 12320, Asuka 12209 and Asuka 881371
114 remained as relict material and were affected by elevated temperature processes. The
115 identification of angrite-like clasts in howardites, various polymict urelites and CH3 chondrites
116 further supports the proposition that the APB was subjected to impact processing^{19,20,21,22}.
117 Moreover, the metal identified within NWA 2999 has been previously attributed to an
118 exogenous source, introduced by impact events²³. Thus, there is a considerable evidence to
119 support impact mixing on the APB early in Solar System history. The lack of shock
120 deformation features within some plutonic, intermediate and dunitic angrites may reflect the
121 greater depth at which these angrites formed or that they were more distal to the impact site
122 (Figure 3). Additionally, the chronological separation between the quenched angrites and
123 plutonic angrites implies that the plutonic angrites were still molten at the time of impact, and
124 therefore did not experience shock induced deformation.

125

126 While mantle rheology has been proposed as the cause of the variable deformation seen
127 in some olivine xenocrysts¹⁴, the oxygen isotopic disequilibrium we observe between the
128 xenocrysts and matrix indicates they have distinct origins, with the matrix the product of an
129 impact event that became contaminated by the impactor, and the olivine xenocrysts
130 representing relict material of the APB. The significant difference in $\Delta^{17}\text{O}$ values, implies that
131 the impactor formed in a different region of the protoplanetary disk in relation to the APB. In
132 a scenario analogous to that proposed from JaH 55617, it would only require a small quantity
133 of impactor material to account for the isotopic disequilibrium displayed by matrix and
134 xenocrysts, provided the impactor carried much more positive $\Delta^{17}\text{O}$ values compared to the
135 APB. It has been recently suggested that angrites record mixing of inner and outer Solar System
136 material (CI and CM carbonaceous chondrites) based on their relatively elevated H and N

137 isotopic compositions^{24,25}. However, the majority of carbonaceous chondrite meteorites
138 reveal negative $\Delta^{17}\text{O}$ values²⁶ and would therefore not induce the more positive matrix values
139 depicted in the quenched angrites. A more viable option would be an ordinary chondrite, which
140 demonstrate positive $\Delta^{17}\text{O}$ values²⁷, however, a chondritic impactor would add high
141 quantities of metal, which is not observed in angrites. It is therefore suggested that the impactor
142 that struck the APB was an achondrite with similar $\Delta^{17}\text{O}$ values to the ordinary chondrites,
143 alike NWA 1104²²⁸. To induce the isotopic difference between the xenocrysts and matrix
144 based on the $\Delta^{17}\text{O}$ composition of NWA 11042 ($\Delta^{17}\text{O} = 1.03\text{‰}$)²⁸, an impactor contribution
145 of less than 10% would be required (see supplementary details).

146

147 Regardless of the impactor, the combination of oxygen isotopic disequilibrium and
148 evidence of high temperature events causing total recrystallization of relict olivine grains,
149 provide a compelling case for mixing early in Solar System history, and an impact melt origin
150 for the quenched angrite meteorites (Figure 3).

151

152 The terrestrial fractionation line (TFL) is commonly used as a graphical reference when
153 comparing distinct groups of extra-terrestrial samples and is normally quoted as having a $\Delta^{17}\text{O}$
154 value of 0‰. However, there is significant uncertainty about the exact $\Delta^{17}\text{O}$ value of the TFL,
155 as this is dependent on the nature of the physical and thermal conditions that affected the
156 reference sample suite used to define it²⁹. In addition, there is, so far no consensus about the
157 appropriate slope factor that should be used for silicate minerals when calculating $\Delta^{17}\text{O}$ ²⁹.
158 Furthermore, it has been shown that terrestrial rocks and minerals form fractionation arrays
159 that display slight y-axis offsets of approximately -30 to -70 ppm on the VSMOW reference
160 scale²⁹. To define an appropriate terrestrial reference line to compare our angrite samples with,
161 we have recalculated the 195 terrestrial samples from a previous study²⁹, using an identical
162 slope value to that used for the angrites (0.5247) and without an applied y-axis offset correction.
163 This reference line is therefore directly comparable with our angrite data and has a $\Delta^{17}\text{O}$ value
164 of $-0.048 \pm 0.020\text{‰}$ (2s). Given that the $\Delta^{17}\text{O}$ value of our newly redefined AFL is $-0.065 \pm$
165 0.017‰ (2s), it is clear that there is overlap between angrites and terrestrial samples (Figure
166 1). This new oxygen isotope evidence therefore supports previous suggestions, made on the
167 basis of pyroxene Fe/Mn ratios, that angrites and terrestrial rocks are derived from a similar
168 primary source reservoir². Although, it is noted that there is a lack of similarity in terms of
169 nucleosynthetic isotopes including $\epsilon^{48}\text{Ca}$, $\epsilon^{50}\text{Ti}$, $\epsilon^{54}\text{Cr}$ and $\epsilon^{62}\text{Ni}$ in addition to severe volatile
170 and alkali depletion in angrites, unlike terrestrial materials^{30,3}.

171 It has been suggested that the formation and migration of giant gas planets are crucial
172 to the evolution of planetary systems, yet the timing of these events in our Solar System remains
173 largely unconstrained³¹. CB chondrites are similarly very ancient meteorites that exhibit
174 evidence of mixing with a differentiated body that could have been sourced from the outer
175 Solar System³¹. It has been subsequently suggested that this extreme dynamical excitement is
176 not an expected result of the classical accretion of bodies, and demands the interference of the
177 giant gas planets³¹.

178

179 There are currently three main competing models to explain the evolution of the Solar
180 System, the ‘Grand Tack’, ‘Low-mass asteroid belt’ and ‘Early Instability models’. However,
181 based on the evidence of large scale mixing, we favour the ‘Grand Tack’. The “Grand Tack”
182 model of giant planet migration implies that Jupiter first migrates inwards and then, as the
183 result of a resonance with Saturn migrated outwards again³². During the initial inward drift,
184 rocky planetesimals were scattered inwards to 1 AU or less. The disc here became thickened
185 and formed the feeder zones for Earth and Venus. However, a proportion (14 %) of these rocky
186 planetesimals were also scattered outwards to 3 AU and beyond. During subsequent outward
187 migration, some of this rocky material was encountered again by the giant planets and scattered
188 back into the inner main disc. Finally, towards the end of the Grand Tack the gas giants moved
189 through the outer icy planetesimal zone, scattering a fraction of them back into the outer main
190 belt³². Based on this model, it is entirely possible that angritic material originating from the
191 same reservoir that formed Earth could have been emplaced into the asteroid belt.

192

193 As previously noted, volcanic activity on the angrite parent body took place extremely
194 early in Solar System history, at around 4564 Ma⁵ and so, approximately 3 Ma after calcium-
195 aluminium-rich inclusion formation (4567.18 ± 0.50 Ma³³). This is within the 4 Ma period in
196 which solar nebular gas is now considered to have persisted³⁴. Impact dynamics within the
197 inner Solar System with gas still present would have been subdued compared to those that
198 prevailed after the nebula had dissipated. As a consequence, displacement of the APB from the
199 inner Solar System and implantation into the main belt appears to have taken place with only
200 low levels of deformation. If this model is correct, it suggests that angrites preserve an early
201 deformation record that is related to Jupiter’s inward and then outwards migration.
202 Consequently, the oxygen isotope disequilibrium recorded by the impact melt and olivine
203 xenocrysts may be the earliest isotopic evidence for the Grand Tack migration.

204

205 **Acknowledgments**

206 Kay Green and Michelle Higgins are thanked for their help in sample preparation.
207 Giulia Degli-Alessandrini is thanked for her assistance with SEM and EBSD analyses. James
208 Malley is thanked for assisting with laser-fluorination work. Graham Ensor is thanked for his
209 help in procuring the NWA angrites. We thank STFC for the studentship awarded to B.G.R-S.
210 L.F.W. is supported by an STFC grant (#ST/P000657/1 & #ST/T000228/1) awarded to MA
211 and IAF. Acquisition and analysis of Asuka 12209 and Asuka 881371 was supported by JSPS
212 KAKENHI (Grant Number 19H01959), NIPR (Research Project KP307), in collaboration with
213 the Belgian Science Policy (Belspo) project BELAM for Asuka 12209. VD, SG and PC thanks
214 the FWO-FNRS Excellence of Science (EoS) programme ET-HoME. VD, LP, SG and PC also
215 thank the Belspo project BELAM for past funding. VD thanks FRS-FNRS for support.

216

217 **Methods**

218 Oxygen isotope analyses were undertaken by laser-assisted fluorination at The Open
219 University, UK following established procedures^{8,15}. Oxygen isotopic analyses are given in
220 standard δ notation, where $\delta^{18}\text{O}$ is calculated relative to the international standard, Vienna
221 Standard Mean Ocean Water (VSMOW) as:

222

$$223 \quad \delta^{18}\text{O} = [({}^{18}\text{O} / {}^{16}\text{O}_{\text{sample}}) / ({}^{18}\text{O} / {}^{16}\text{O}_{\text{VSMOW}}) - 1] \times 1000 (\text{‰})$$

224

225 and similarly, for $\delta^{17}\text{O}$ using the ${}^{17}\text{O} / {}^{16}\text{O}$ ratio.

226

227 $\Delta^{17}\text{O}$ represents the deviation of a sample, or group of samples, from the terrestrial
228 fractionation line (TFL) and has proved to be a useful parameter for defining different parent
229 body sources^{15,35} In this paper all $\Delta^{17}\text{O}$ were calculated using the linearized format³⁵ with $\lambda =$
230 0.5247.

231

$$232 \quad \Delta^{17}\text{O} = 1000 \ln(1 + \delta^{17}\text{O}/1000) - \lambda 1000 \ln(1 + \delta^{18}\text{O}/1000)$$

233

234 In this paper all $\Delta^{17}\text{O}$ were calculated using the linearized format³⁶.

235

236 Laser-assisted fluorination currently provides the highest precision available for
237 oxygen isotope analysis. Replicate analyses of our internal obsidian standard (N = 38) gave the
238 following values: (2SD) of $\pm 0.053\text{‰}$ ($\delta^{17}\text{O}$), $\pm 0.095\text{‰}$ ($\delta^{18}\text{O}$), and $\pm 0.018\text{‰}$ ($\Delta^{17}\text{O}$)³⁷. While

239 laser fluorination does not provide spot analysis, unlike secondary ion mass spectrometry
240 (SIMS) or UV laser ablation, the need to resolve slight differences in $\Delta^{17}\text{O}$ means that it is the
241 most suitable technique for this study.

242

243 Olivine grains were carefully plucked from the matrix using sterile tweezers. Following
244 the separation, whole rock samples along with matrix and olivine-rich fractions of NWA
245 12320, Asuka 12209 and Asuka 881371 (~2 mg of material per replicate) were loaded into
246 separate wells in a Ni sample holder. Once the fractions were loaded, the tray was placed in
247 the sample chamber. The sample chamber was next brought down to a vacuum pressure of 10^{-7}
248 mbar. Heater tape was then wrapped around the sample chamber and it was baked out at
249 around 80 °C overnight to remove any adsorbed moisture from the system that could affect the
250 oxygen isotope analyses.

251

252 An internal obsidian standard was run with the samples to monitor accuracy and
253 precision. During laser heating, the beam diameter was initially set at 3 mm and the laser power
254 slowly increased to a maximum of 20 W. In order to complete the reaction, the beam diameter
255 was reduced to 1 mm and the laser power increased rapidly to a maximum value of 14 W. This
256 second step ensures that any residual material that may have been missed from the first phase
257 is fully reacted. Following the reaction of the sample, the gas is expanded into a
258 ThermoFinnigan MAT 253 Dual Inlet Isotope Ratio Mass Spectrometer (IRMS).

259

260 Unlike other meteorite groups, angrites have very few recorded falls (with Angra Dos
261 Reis being the only recorded fall)³. Despite the long terrestrial residence times for angrite
262 meteorites, which range from <0.06 to 0.43 Ma, terrestrial contamination is minor³. On hand
263 specimen examination, some of the Northwest Africa finds appear to be moderately weathered.
264 This can present a significant problem when attempting to obtain high levels of precision
265 during oxygen isotope analyses. To resolve this issue, leaching of meteoritic finds can remove
266 weathering products, mitigating terrestrial contamination. In this study, we analysed chips of
267 both untreated material and leached material (70 – 170 mg) to determine whether or not the
268 angrites investigated had indeed been affected by terrestrial alteration. This process was
269 conducted using a solution of ethanolamine thioglycollate (EATG). Tests undertaken on a suite
270 of variably weathered H chondrites indicated that the EATG-wash method was efficient at
271 removing Fe-rich alteration products, without disturbing the primary oxygen isotope
272 composition of the samples³⁸. EATG treatment is preferred in comparison to conventional

273 leaching in dilute HCl, as this method can partially remove indigenous glass and feldspathic-
274 rich material. Each meteorite investigated in this project was weighed and placed into
275 centrifuge tubes. Between ~4 and ~12 ml of EATG was added to the tubes using a pipette and
276 shaken to separate the sample into the solution (mixing repeated every 10 mins for 2 hrs). Once
277 the sample has fully reacted with the EATG, the waste EATG is removed and replaced with
278 50/50 isopropanol alcohol (IPA) and deionized water. This new mixture is shaken four times
279 to ensure the entirety of the sample is treated. The last step is to remove the mixture and replace
280 with straight IPA and mix in the centrifuge for a few minutes. The sample is then removed
281 from the IPA and left to evaporate in ambient temperatures. The weighed, treated samples are
282 then investigated using the same methodology as the untreated samples.

283

284 A small chip of NWA 12320 was embedded within a 1-inch round e-poxy mount and
285 coated using a Safematic CCU-010 Compact Coating Unit (<5 μm). The mount was then
286 subsequently investigated using a Zeiss Crossbeam 550 with an Oxford Instruments Symmetry
287 2 EBSD detector at The Open University. High resolution Energy Dispersive X-Ray
288 Spectroscopy (EDS) smart-mapping was collected using an Oxford Instruments Ultim Extreme
289 and an Oxford Instruments Ultim Max detector. The sample was tilted to 70° and an electron
290 beam was used to generate EBSD “maps”, consisting of electron backscatter diffraction
291 patterns (EBSPs) acquired at step-sizes ranging from 400 nm. The beam conditions used for
292 both EDS and EBSD analyses comprised an incident beam ranging between 1-2 nA current
293 and a 20 kV accelerating voltage at a working distance of 12 mm.

294

295 **Data availability**

296 All data used in the manuscript are presented in the Supplementary Data and are
297 available on request from the corresponding author.

298

299 **References**

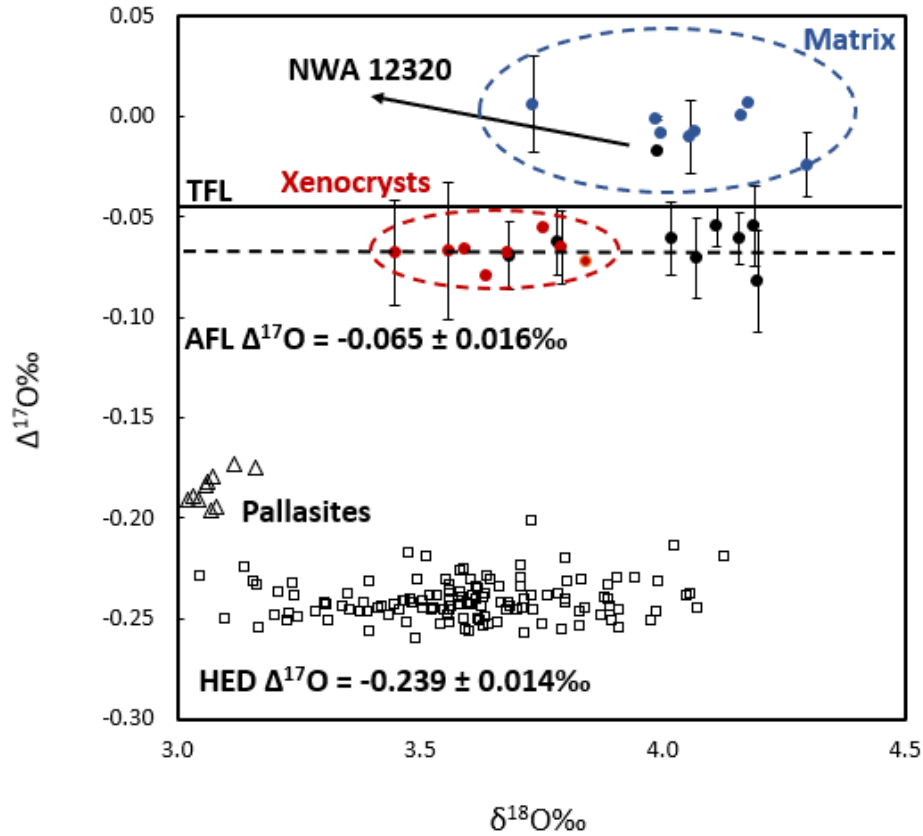
- 300 1. Kruijer, T. S., Kleine, T., & Borg, L. E. The great isotopic dichotomy of the early Solar
301 System. *Nature Astronomy* (2019). <https://doi.org/10.1038/s41550-019-0959-9>
302 2. Papike, J. J., Burger, P. V., Bell, A. S., & Shearer, C. K. Mn-Fe systematics in major
303 planetary body reservoirs in the solar system and the positioning of the Angrite Parent
304 Body: A crystal-chemical perspective. *American Mineralogist*. 102, 1759-1762 (2017).
305 <https://doi.org/10.2138/am-2017-6112>

- 306 3. Keil, K. Angrites, a small but diverse suite of ancient, silica-undersaturated volcanic-
307 plutonic mafic meteorites, and the history of their parent asteroid. *Chemie der Erde*.
308 72.191-218 (2012). <https://doi.org/10.1016/j.chemer.2012.06.002>
- 309 4. Mittlefehldt, D. W., Killgore, M., & Lee, M. T. Petrology and geochemistry of D'Orbigny,
310 geochemistry of Sahara 99555 and the origin of Angrites. *Meteoritics and Planetary*
311 *Science*. 37, 345-369 (2002). <https://doi.org/10.1111/j.1945-5100.2002.tb00821.x>
- 312 5. Zhu, K., Moynier, F., Wielandt, D., Larsen, K. K., Barrat, J. A., & Bizzarro, M. Timing and
313 Origin of the Angrite Parent Body Inferred from Cr Isotopes. *The Astrophysical Journal*
314 *Letters*. 887: L13 (2019). <https://doi.org/10.3847/2041-8213/ab2044>
- 315 6. Santos, A. R., Agee, C. B., Shearer, C. K., & McCubbin, F. M. Northwest Africa 8535 and
316 Northwest Africa 10463: New insights into the Angrite parent body. 47th Lunar and
317 *Planetary Science Conference*. Abstract #2590 (2016).
- 318 7. Reger, P. M., Zhang, B., Gannoun, A. M., Regelous, M., Agee, C. B., & Bouvier, A.
319 Chronology of the unique Angrite Northwest Africa 10463. 84th Annual Meeting of The
320 *Meteoritical Society*. Abstract #2609. (2021).
- 321 8. Greenwood, R. C., Franchi, I. A., Jambon, A., & Buchanan, P. C. Widespread magma oceans
322 on asteroidal bodies in the early Solar System. *Nature*. 435, 916-918 (2005).
323 <https://doi.org/10.1038/nature03612>
- 324 9. Greenwood, R. C., Burbine, T. H., Miller, M. F., & Franchi, I. A. Melting and differentiation
325 of early-formed asteroids: The perspective from high precision oxygen isotope studies.
326 *Chemie der Erde*. 77, 1-43 (2017). <https://doi.org/10.1016/j.chemer.2016.09.005>
- 327 10. Scott, E. R. D., & Bottke, W. F. Impact histories of Angrites, eucrites and their parent
328 bodies. *Meteoritics and Planetary Science*. 46 (12), 1878-1887 (2011).
329 <http://dx.doi.org/10.1111/j.1945-5100.2011.01301.x>
- 330 11. Jambon, A., Barrat, J. A., Boudouma, O., Fonteilles, M., Badia, D., Göpel, C., & Bohn, M.
331 Mineralogy and petrology of the Angrite Northwest Africa 1296. *Meteoritics and*
332 *Planetary Science*. 40, 361-375 (2005). [https://doi.org/10.1111/j.1945-](https://doi.org/10.1111/j.1945-5100.2005.tb00388.x)
333 [5100.2005.tb00388.x](https://doi.org/10.1111/j.1945-5100.2005.tb00388.x)
- 334 12. Jambon, A., Boudouma, O., Fonteilles, M., Guillou, C. L., Badia, D., & Barrat, J. A.
335 Petrology and mineralogy of the Angrite Northwest Africa 1670. *Meteoritics and*
336 *Planetary Science*. 43, 1783-1795 (2008). [https://doi.org/10.1111/j.1945-](https://doi.org/10.1111/j.1945-5100.2008.tb00643.x)
337 [5100.2008.tb00643.x](https://doi.org/10.1111/j.1945-5100.2008.tb00643.x)
- 338 13. Mikouchi, T., Hasegawa, H., Takenouchi, A., & Kagi, H. Olivine xenocrysts in Asuka-
339 881371 revisited. 46th Lunar and Planetary Science Conference. Abstract #2065 (2015).

- 340 14. Mikouchi, T., Yamaguchi, A., Debaille, V., McKibbin, S., Goderis, S., Pittarello, L., Shirai,
341 N., Hublet, G., Quitté, G., Iizuka, T., Greenwood, R. C., & Claeys, P. Mineralogy of
342 olivine xenocrysts in Asuka 12009 angrite. 48th Lunar and Planetary Science
343 Conference. Abstract #2206 (2017).
- 344 15. Miller, M. F., Franchi, I. A., Sexton, A. S., & Pillinger, C. T. High Precision $\delta^{17}\text{O}$ Isotope
345 Measurements of Oxygen from Silicates and Other Oxides: Method and Applications.
346 Rapid Communications in Mass Spectrometry. 13, 1211-1217 (1999).
347 [https://doi.org/10.1002/\(SICI\)1097-0231\(19990715\)13:13%3C1211::AID-
348 RCM576%3E3.0.CO;2-M](https://doi.org/10.1002/(SICI)1097-0231(19990715)13:13%3C1211::AID-RCM576%3E3.0.CO;2-M)
- 349 16. Trepmann, C. A., Renner, J., & Druiventak, A. Experimental deformation and
350 recrystallization of olivine – processes and timescales of damage healing during
351 postseismic relaxation at mantle depths. Solid Earth Discussions. 5, 463-524 (2013).
352 <https://doi.org/10.5194/se-4-423-2013>
- 353 17. Janots, E., Gnos, E., Hofmann, B. A., Greenwood, R. C., Franchi, I. A., Bermingham, K.,
354 & Netwing, V. Jiddat al Harris 556: A howardite impact melt breccia with an H
355 chondrite component. Meteoritics and Planetary Science. 47, 1558-1574 (2012).
356 <https://doi.org/10.1111/j.1945-5100.2012.01419.x>
- 357 18. Janots, E., Gnos, E., Hofmann, B. A., Greenwood, R. C., Franchi, I. A., & Bischoff, A.
358 Jiddat al Harris 422: A ureilite with an extremely high degree of shock melting.
359 Meteoritics and Planetary Science. 46, 134-148 (2011). [https://doi.org/10.1111/j.1945-
360 5100.2010.01161.x](https://doi.org/10.1111/j.1945-5100.2010.01161.x)
- 361 19. Nazarov, M. A., Brandstätter, F., & Kurat, G. Angrite-like clasts from the Erevan
362 howardite. Abstract. 1033-1034 (1995).
- 363 20. Cohen, B. A., Goodrich, C. A., & Keil, K. Feldspathic clast populations in polymict
364 ureilites: Stalking the missing basalts from the ureilite parent body. Geochimica et
365 Cosmochimica Acta. 64 (20), 4249-4266 (2004).
366 <https://doi.org/10.1016/j.gca.2004.01.027>
- 367 21. Kita, N. T., Ikeda, Y., Togashi, S., Liu, Y., Morishita, Y., & Weisberg, M. K. Origin of
368 ureilites, inferred from a SIMS oxygen isotopic and trace element study of clasts in the
369 Dar al Gani polymict ureilites. Geochimica et Cosmochimica Acta. 68 (20), 4213-4235
370 (2004). <https://doi.org/10.1016/j.gca.2004.03.020>
- 371 22. Zhang, A. C., Kawasaki, N., Kuroda, M., Li, Y., Wang, H. P., Bai, X. N., Sakamoto, N.,
372 Yin, Q. Z., Yurimoto, H. Unique angrite-like fragments in a CH3 chondrite reveal a

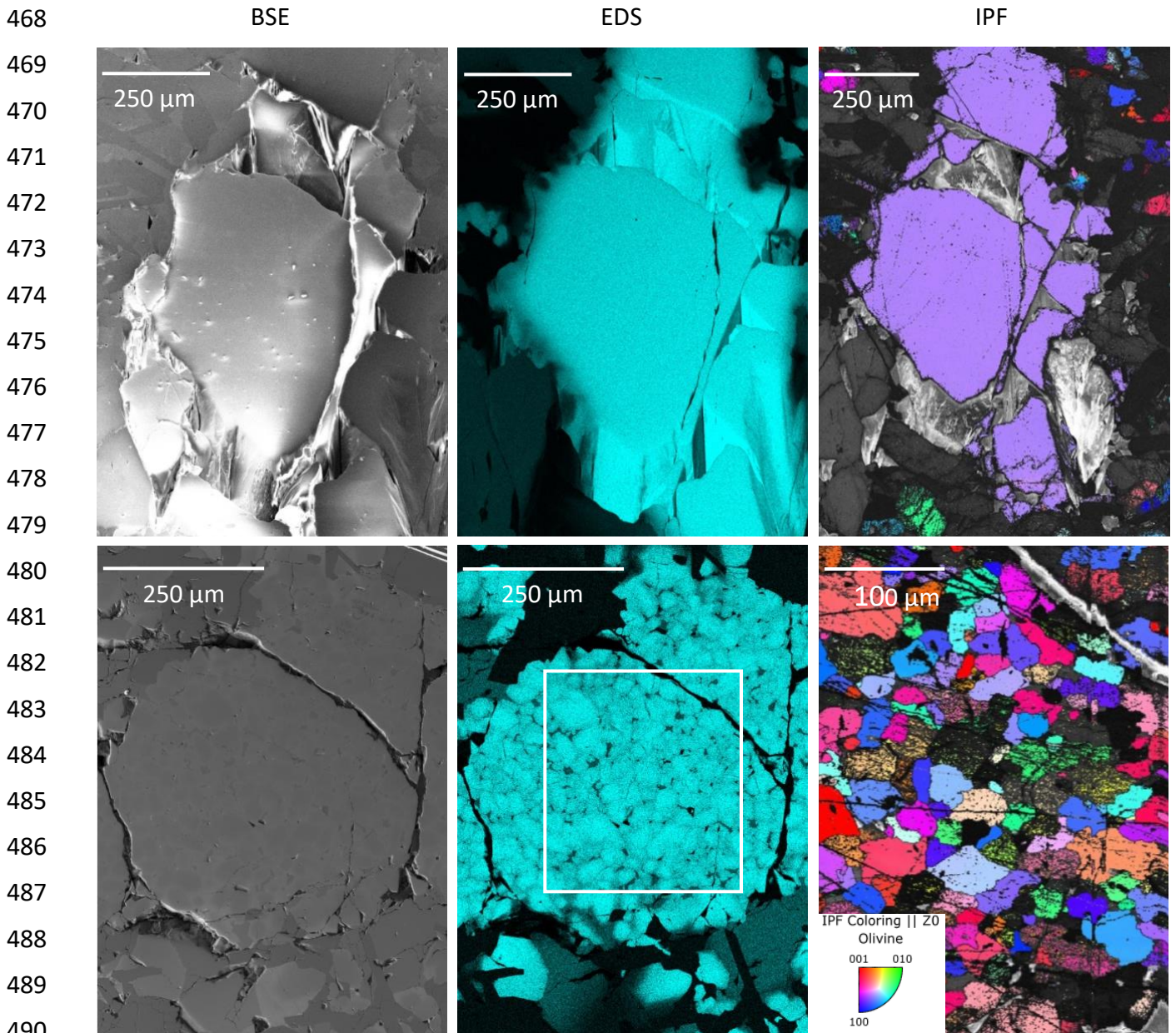
- 373 new basaltic planetesimal. *Geochimica et Cosmochimica Acta*. 275, 48-63 (2020).
374 <https://doi.org/10.1016/j.gca.2020.02.014>
- 375 23. Jambon, A., Baghdadi, B., & Barrat, J. A. Peridotitic angrites are chimerolites. 43rd Lunar
376 and Planetary Science Conference. Abstract #1758 (2012).
- 377 24. Sarafian, A. R., Hauri, E. H., McCubbin, M., Lapen, T. J., Berger, E. L., Nielson, S. G.,
378 Marschall, H. R., Gaetani, G. A., Righter, K., & Sarafian E. Early accretion of water
379 and volatile elements to the inner Solar System: evidence from angrites. *Philosophical*
380 *Transactions of the Royal Society*. 375. <https://doi.org/10.1098/rsta.2016.0209>
- 381 25. Deligny, C., Füre, E., & Deloule E. Origin and timing of volatile delivery (N, H) to the
382 angrite parent body: Constraints from in situ analyses of melt inclusions. *Geochimica*
383 *et Cosmochimica Acta*. 313, 243-256 (2021).
384 <https://doi.org/10.1016/j.gca.2021.07.038>
- 385 26. Greenwood, R. C., Burbine, T. H., & Franchi, I. A. Linking asteroids and meteorites to the
386 primordial planetesimal population. *Geochimica et Cosmochimica Acta*. 277, 377-406
387 (2020). <https://doi.org/10.1016/j.gca.2020.02.004>
- 388 27. Clayton, R. N., Mayeda, T. K., Goswami, J. N., & Olsen, E. J. Oxygen isotope studies of
389 ordinary chondrites. *Geochimica et Cosmochimica Acta*. 55, 2317-2337 (1991).
390 [https://doi.org/10.1016/0016-7037\(91\)90107-G](https://doi.org/10.1016/0016-7037(91)90107-G)
- 391 28. Vaci, Z., Agee, C. B., Humayun, M., Ziegler, K., Asmerom, Y., Polyak, V., Busemann, H.,
392 Krietsch, D., Heizler, M., Sanborn, M. E., & Yin, Q. Z. Unique achondrite Northwest
393 Africa 11042: Exploring the melting and breakup of the L chondrite parent body.
394 *Meteoritics and Planetary Science*. 55, 622-648 (2020).
395 <https://doi.org/10.1111/maps.13456>
- 396 29. Greenwood R. C., Barrat J-A., Miller M. F., Anand A., Dauphas N., Franchi I. A., Sillard
397 P. and Starkey N. A. Oxygen isotopic evidence for accretion of Earth's water before a
398 high-energy Moon-forming giant impact. *Science Advances*. 4, 3 (2018).
399 <https://doi.org/10.1126/sciadv.aao5928>
- 400 30. Qin, L. & Carlson, R. W. Nucleosynthetic isotope anomalies and their cosmochemical
401 significance. *Geochemical Journal*. 50, 43-65 (2016).
402 <https://doi.org/10.2343/geochemj.2.0401>
- 403 31. Johnson, B. C., Walsh, K. J., Minton, D. A., Krot, A. N., & Levison, H. F. Timing of the
404 formation and migration of giant planets as constrained by CB chondrites. *Science*
405 *Advances*, 2, 12 (2016). <https://doi.org/10.1126/sciadv.1601658>

- 406 32. Walsh, K., Morbidelli, A., Raymond, S., O'Brien, D. P., & Mandell, A. M. A low mass for
407 Mars from Jupiter's early gas-driven migration. *Nature*. 475, 206–209 (2011).
408 <https://doi.org/10.1038/nature10201>
- 409 33. Amelin, Y., Kaltenbach, A., Iizuka, T., Stirling, C. H., Ireland, T. R., Petaev, M., &
410 Jacobsen, B. S. U-Pb chronology of the Solar System's oldest solids with variable
411 $^{238}\text{U}/^{235}\text{U}$. *Earth and Planetary Science Letters*. 300 (3-4), 343-350 (2010).
412 <https://doi.org/10.1016/j.epsl.2010.10.015>
- 413 34. Wang, H., Weiss, B. P., Bai, X. N., Downey, B. G., Wang, J., Wang, J., Suavet, C., Fu, R.,
414 R., & Zucolotto, M. E. Lifetime of the solar nebula constrained by meteorite
415 paleomagnetism. *Science* 355, 623-627 (2017).
416 <https://doi.org/10.1126/science.aaf5043>
- 417 35. Clayton, R. N., & Mayeda, T. K. Oxygen isotope studies of Achondrites. *Geochimica et*
418 *Cosmochimica Acta*. 60, 1999-2017 (1996). [https://doi.org/10.1016/0016-](https://doi.org/10.1016/0016-7037(96)00074-9)
419 [7037\(96\)00074-9](https://doi.org/10.1016/0016-7037(96)00074-9)
- 420 36. Miller, M. F. Isotopic fractionation and the quantification of ^{17}O anomalies in the oxygen
421 three-isotope system: an appraisal and geochemical significance. *Geochimica et*
422 *Cosmochimica Acta*. 66, 1881–1889 (2002). [https://doi.org/10.1016/S0016-](https://doi.org/10.1016/S0016-7037(02)00832-3)
423 [7037\(02\)00832-3](https://doi.org/10.1016/S0016-7037(02)00832-3)
- 424 37. Starkey, N. A., Jackson, C. R. M., Greenwood, R. C., Parman, S., Franchi, I., Jackson, M.,
425 Fritton, J. G., Stuart, F. M., Kurz, M., & Larsen, L. M. Triple oxygen isotopic
426 composition of the high $^3\text{He}/^4\text{He}$ mantle. *Geochimica et Cosmochimica Acta*. 176, 227-
427 238 (2016). <https://doi.org/10.1016/j.gca.2015.12.027>
- 428 38. Martins, Z., Hofmann, B. A., Gnos, E., Greenwood, R. C., Verchovsky, A., Franchi, I., Jull,
429 A. J. T., Botta, O., Glavin, D. P., Dworkin, J. P., Ehrenfreund, P. Amino acid
430 composition, petrology, geochemistry, ^{14}C terrestrial age and oxygen isotopes of the
431 Shisr 033 CR chondrite. *Meteoritics & Planetary Science*. 42 (9), 1581-1595 (2010).
432 <https://doi.org/10.1111/j.1945-5100.2007.tb00592.x>
433



434
 435
 436
 437
 438
 439
 440
 441
 442
 443
 444
 445
 446
 447
 448
 449
 450
 451
 452
 453
 454
 455
 456
 457
 458
 459
 460
 461
 462
 463
 464
 465
 466
 467

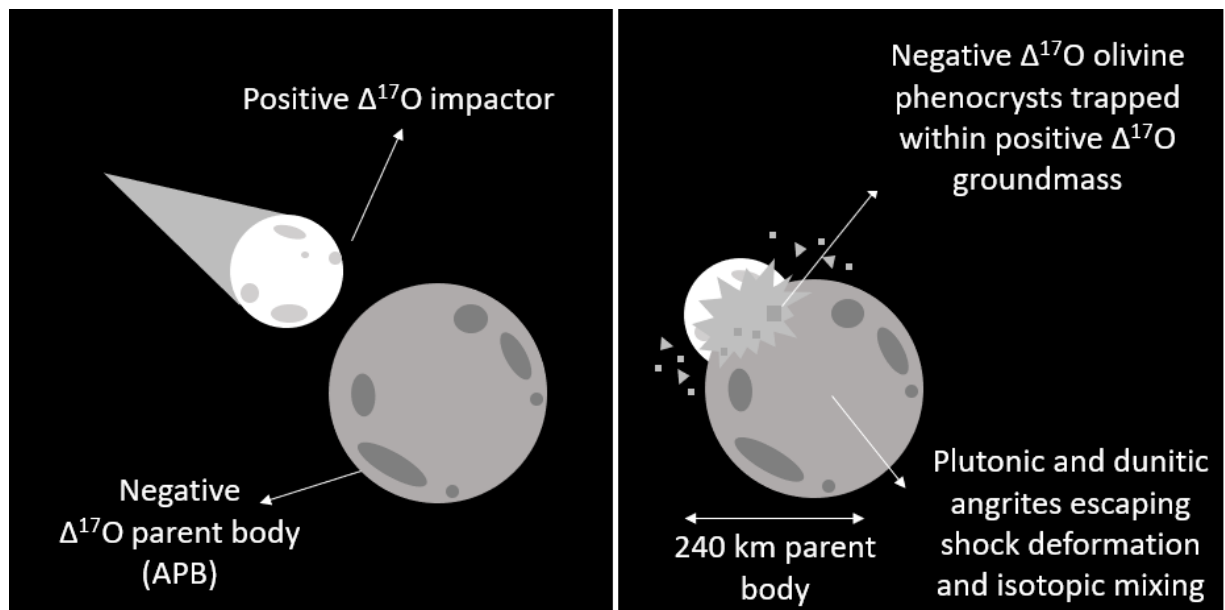
Figure 1: Triple oxygen isotope systematics for angrites, pallasites and HEDs. In this diagram we show our angrite data in relation to a TFL line that has been calibrated using a suite of 195 terrestrial samples run under identical conditions to the angrites in this study and calculated using the same slope factor (0.5247) (see text for further details). The fact that our newly defined AFL shows significant overlap with this terrestrial reference line at the 2 σ level supports suggestions that the APB and Earth formed from the same reservoir. Our data are consistent with the possibility that angrites may represent material from the giant Moon-forming impactor. Olivine xenocrysts from Asuka 12209, Asuka 881371 and NWA 12320 display similar values to bulk angrites (black closed circles) and fall within the newly-defined angrite fractionation line ($\Delta^{17}\text{O} -0.065 \pm 0.017\text{‰}$), while matrix fractions yield more positive $\Delta^{17}\text{O}$ values. This discrepancy in at least three angritic meteorites, suggests unique parent bodies for both the olivine and matrix fractions, requiring early mixing of planetary reservoirs on the angrite parent body. The angrite meteorites are well resolved from both pallasite meteorites (black triangles) and howardite-eucrite-diogenite (HED) meteorites (black squares)⁷.



492 **Figure 2: Chemical and structural characterisation of olivine xenocrysts in NWA 12320.**
 493 *Two populations of xenocrysts are observed within the sample, with chemically heterogenous*
 494 *recrystallized olivine occurring in close proximity to undeformed grains. Given the low state*
 495 *of deformation within both the undeformed olivine xenocrysts, as well as the majority of angrite*
 496 *meteorites, olivine recrystallization for a subset of xenocrysts must have occurred prior to*
 497 *crystallization of the bulk sample, suggesting that the olivine xenocrysts are relict material that*
 498 *survived impact melting.*

499
500
501

502
503
504
505
506
507
508
509
510
511
512
513
514



515 *Figure 3 – A schematic depicting a possible scenario which causes the oxygen isotopic*
516 *disequilibrium in the quenched angrite meteorites. An impactor with a positive oxygen*
517 *isotopic composition, collides with the angrite parent body (APB). Mixing of the two separate*
518 *bodies occurs and relict olivine grains of the APB are affected by high temperature events.*
519 *Plutonic and dunitic angrites escape shock deformation and isotopic mixing due to their depth/*
520 *distance from the impact site on the APB or due to being molten during the time of impact*
521 *mixing.*